COMISIÓN NACIONAL DE BANCOS Y SEGUROS

WORKING PAPER:

Dynamic financial processes identification using sparse regressive reservoir computers

AUTHORS

Fredy Vides
Idelfonso B. R. Nogueira
Lendy Banegas
Evelyn Flores

October 18, 2023

Dynamic financial processes identification using sparse regressive reservoir computers

Fredy Vides,[1, 2, a)] Idelfonso B. R. Nogueira,[3, b)] Lendy Banegas,[1, c)] and Evelyn Flores[1, d)]
[1)]*Department of Statistics and Research, National Commission of Banks and Insurance Companies of Honduras, Honduras*
[2)]*Department of Applied Mathematics, Universidad Nacional Autónoma de Honduras, Honduras*
[3)]*Department of Chemical Engineering, Norwegian University of Science and Technology, Norway*

(Dated: October 18, 2023)

In this document, we present key findings in structured matrix approximation theory, with applications to the regressive representation of dynamic financial processes. Initially, we explore a comprehensive approach involving generic nonlinear time delay embedding for time series data extracted from a financial or economic system under examination. Subsequently, we employ sparse least-squares and structured matrix approximation methods to discern approximate representations of the output coupling matrices. These representations play a pivotal role in establishing the regressive models corresponding to the recursive structures inherent in a given financial system. The document further introduces prototypical algorithms that leverage the aforementioned techniques. These algorithms are demonstrated through applications in approximate identification and predictive simulation of dynamic financial and economic processes, encompassing scenarios that may or may not exhibit chaotic behavior.

The intricate dynamics inherent in financial processes often pose challenges for accurate modeling and prediction. Nonetheless, the synergy of sparse representation techniques with Nonlinear Regressive Reservoir Computers (NRRCs) proves advantageous in modeling financial processes dynamics. Firstly, this approach excels in capturing the intricate nonlinear dynamics of financial data. NRRCs, adept at modeling complex relationships between input and output data, coupled with sparse representation, effectively identify the key dynamic components, ensuring more accurate and precise modeling of underlying dynamics. Secondly, the methodology promotes efficient data utilization. NRRCs, capable of learning from a relatively small dataset, align well with the limited scope and complexity of financial processes data. By pinpointing crucial variables, the approach enhances modeling efficiency, conserving time and resources. Thirdly, the approach exhibits flexibility and adaptability. NRRCs swiftly respond to changing conditions, making them ideal for the dynamic nature of financial processes. The amalgamation of NRRCs with sparse representation facilitates the identification of changes in the underlying structure, enabling prompt adjustments to the model. In conclusion, integrating sparse representation techniques with time series models employing nonlinear regressive reservoir computers yields several advantages for financial processes dynamics modeling. It ensures accurate modeling of complex dynamics, optimizes data utilization, and provides adaptability to evolving conditions.

[a)]Electronic mail: fredy.vides@cnbs.gob.hn
[b)]Electronic mail: idelfonso.b.d.r.nogueira@ntnu.no
[c)]Electronic mail: lendy.banegas@cnbs.gob.hn
[d)]Electronic mail: evelyn.flores@cnbs.gob.hn

I. INTRODUCTION

Regressive models and reservoir computers are robust computational tools for the identification and simulation of financial and economic systems[4]. In recent years, a new class of architectures, termed next-generation reservoir computers, has emerged[10]. In this study, we delve into the intrinsic network architecture associated with these reservoir computers, which significantly contribute to data dimensionality reduction. This architecture also facilitates the parametric identification processes by leveraging the matrix structural constraints induced by the network architecture. The document outlines key aspects of the theory and algorithms pertaining to the computation of specific types of regressive reservoir computers. The focus of this study is on reservoir computers, the architecture of which can be approximated by either linear or nonlinear regressive vector models.

The main contribution of the work reported in this document is the application of *collaborative schemes* involving structured matrix approximation methods, together with linear and nonlinear regressive models, to the simulation of dynamic financial processes. Some theoretical aspects of the aforementioned methods are described in §III. As a byproduct of the work reported in this document, a toolset of Python programs for financial and economic dynamic models identification based on the ideas presented in §III and §IV has been developed and is available in[15].

Even though, the applications of the structure preserving function approximation technology developed as part of the work reported in this document can range from numerical modeling of cyber-physical systems[16], to climate simulation[13]. We will focus on applications to financial processes identification in this paper.

Financial processes have become complex systems where several dynamic entities constantly communicate and affect each other. Hence, the financial processes identification has become a critical aspect of modern finance. The identified

models can become a helpful tool for institutions to analyze and predict financial trends, manage risk, and make informed investment decisions (Bodie et al., 2014). However, the complexity and uncertainty of financial markets make these tasks challenging. Financial processes often exhibit nonlinear and complex behavior, which makes it difficult to model and identify the underlying dynamics (Cont, 2001). Traditional linear models may fail to capture the intricate relationships between variables, leading to inaccurate predictions and suboptimal decision-making.

Despite the challenges posed by the factors described above, data quality, and market efficiency, machine learning techniques offer promising solutions for improving the accuracy and utility of financial models. Machine learning has been used to identify the relationship between the key financial ratios that characterize a firm's financial position. For instance, Dixon, Klabjan, and Bang's[9] work applies deep learning to predict financial market movements. The authors use a classification approach to predict financial market movements. Their findings suggest that deep learning algorithms can provide valuable insights and predictions about financial market movements, outperforming traditional methods. Sirignano and Cont[14] propose a deep learning model to identify the dynamics of price formation of a high-frequency limit order book. Their model was able to capture universal features of price formation across different markets, highlighting the potential of machine learning to model complex financial systems.

Overall, the recent literature suggests that machine learning has significant potential in modeling financial data. These techniques are increasingly utilized to capture complex patterns, make accurate predictions, and optimize decision-making in the financial domain. However, it is still an open issue to be investigated. In this scenario, this work also contributes to the field of financial data identification by applying the proposed tools in this context leading to a better understanding of the underlying financial processes addressed here.

A prototypical algorithm for the computation of sparse structured recursive models based on the ideas presented in §III, is presented in §IV. Some numerical simulations of financial processes based on the prototypical algorithm presented in §IV are documented in §V.

II. PRELIMINARIES AND NOTATION

The symbols $\mathbb{R}^+$ and $\mathbb{Z}^+$ will be used to denote the positive real numbers and positive integers, respectively. For any pair $p,n\in\mathbb{Z}^+$ the expression $d_p(n)$ will denote the positive integer $d_p(n)=n(n^p-1)/(n-1)+1$. Given $\delta>0$, let us consider the function defined by the expression

$$H_\delta(x)=\begin{cases}1, & x>\delta\\ 0, & x\leq\delta\end{cases}.$$

Given a matrix $A\in\mathbb{C}^{m\times n}$ with singular values[11] (§2.5.3) denoted by the expressions $s_j(A)$ for $j=1,\ldots,\min\{m,n\}$. We will write $\mathrm{rk}_\delta(A)$ to denote the number

$$\mathrm{rk}_\delta(A)=\sum_{j=1}^{\min\{m,n\}}H_\delta(s_j(A)).$$

For a nonzero matrix $A\in\mathbb{R}^{m\times n}$, the symbol A^+ will be used to denote the pseudoinverse[11] (§5.5.4) of A.

Given a scalar time series $\Sigma=\{x_t\}_{t\geq 1}\subset\mathbb{R}^\kappa$, a positive integer L and any $t\geq L$, we will write $\mathbf{x}_L(t)$ to denote the vector

$$\mathbf{x}_L(t)=\begin{bmatrix}\mathbf{x}_L^{(1)}(t)^\top & \mathbf{x}_L^{(2)}(t)^\top & \cdots & \mathbf{x}_L^{(n)}(t)^\top\end{bmatrix}^\top\in\mathbb{R}^{nL},$$

with

$$\mathbf{x}_L^{(j)}(t)=\begin{bmatrix}x_{t-L+1}^{(j)} & x_{t-L+2}^{(j)} & \cdots & x_{t-1}^{(j)} & x_t^{(j)}\end{bmatrix}^\top\in\mathbb{R}^L.$$

for $1\leq j\leq n$, where $x_{j,s}$ denotes the scalar j-component of each element x_s in the vector time series Σ, for $s\geq 1$.

The identity matrix in $\mathbb{R}^{n\times n}$ will be denoted by I_n, and we will write $\hat{e}_{j,n}$ to denote the matrices in $\mathbb{R}^{n\times 1}$ representing the canonical basis of $\mathbb{R}^n$ (each $\hat{e}_{j,n}$ corresponds to the j-column of I_n). For any vector $x\in\mathbb{R}^n$, we will write $\|x\|$ to denote the Euclidean norm of x. Given a matrix $X\in\mathbb{R}^{m\times n}$, the expression $\|X\|_F$ will denote the Frobenius norm of X.

For any integer $n>0$, in this article, we will identify the vectors in $\mathbb{R}^n$ with column matrices in $\mathbb{R}^{n\times 1}$.

Given two matrices $A\in\mathbb{R}^{m\times n}$, $B\in\mathbb{R}^{p\times q}$, the tensor Kronecker tensor product $A\otimes B\in\mathbb{R}^{mp\times nq}$ is determined by the following operation.

$$A\otimes B=\begin{bmatrix}a_{11}B & \cdots & a_{1n}B\\ \vdots & \ddots & \vdots\\ a_{m1}B & \cdots & a_{mn}B\end{bmatrix}$$

For any integer $p>0$ and any matrix $X\in\mathbb{R}^{m\times n}$, we will write $X^{\otimes p}$ to denote the operation determined by the following expression.

$$X^{\otimes p}=\begin{cases}X & ,p=1\\ X\otimes X^{\otimes(p-1)} & ,p\geq 2\end{cases}$$

We will also use the symbol Π_p to denote the operator $\Pi_p:\mathbb{R}^n\to\mathbb{R}^{n^p}$ that is determined by the expression $\Pi_p(x):=x^{\otimes p}$, for each $x\in\mathbb{R}^n$.

For any matrix $A\in\mathbb{R}^{m\times n}$, we will denote by $\mathrm{colsp}(A)$ the columns space of the matrix A. Given a list $A_1,A_2,\ldots,A_m$ such that for $1\leq j\leq m$, $A_j\in\mathbb{R}^{n_j\times n_j}$ for some integer $n_j>0$. The expression $A_1\oplus A_2\oplus\cdots\oplus A_m$ will denote the block diagonal matrix

$$A_1\oplus A_2\oplus\cdots\oplus A_m=\begin{bmatrix}A_1 & & & \\ & A_2 & & \\ & & \ddots & \\ & & & A_m\end{bmatrix},$$

where the zero matrix blocks have been omitted.

In this article, we will use the following notion of sparse representation. Given $\delta>0$ and two matrices $A\in\mathbb{R}^{m\times n}$ and

$X \in \mathbb{R}^{n\times p}$, a matrix $\hat{X} \in \mathbb{R}^{n\times p}$ is an approximate sparse representation of X with respect to A, or a sparse representation of X for short, if $\|\hat{X}A - XA\|_F \leq C\delta$ for some $C > 0$ that does not depend on δ, and $\hat{X}$ has fewer nonzero entries than X.

We will write $\mathbf{S}^1$ to denote the set $\{z \in \mathbb{C} : |z| = 1\}$. Given any matrix $X \in \mathbb{R}^{m\times n}$, we will write $X^\top$ to denote the transpose $X^\top \in \mathbb{R}^{n\times m}$ of X. A matrix $P \in \mathbb{C}^{n\times n}$ will be called an orthogonal projector whenever $P^2 = P = P^\top$. Given any matrix $A \in \mathbb{R}^{n\times n}$, we will write $\Lambda(A)$ to denote the spectrum of A, that is, the set of eigenvalues of A.

III. STRUCTURED DYNAMIC TRANSFORMATION MODEL IDENTIFICATION

Given two discrete-time dynamic systems determined by two time series $\{x_t\}_{t\geq 1}$ and $\{y_t\}_{t\geq 1}$, respectively. We will study the identification process of maps determined by the expression

$$y_t = \mathscr{F}(x_t) + r_t, \tag{III.1}$$

where $\{r_t\}_{t\geq 1}$ denotes the sequence of residual errors determined for each $t \geq 1$ by $r_t := \|x_t - \mathscr{F}(x_t)\|$ for some suitable norm $\|\cdot\|$.

A. Low-rank approximation and sparse linear least squares solvers

In this section, some low-rank approximation methods with applications to the solution of sparse linear least squares problems are presented.

Definition III.1. *Given $\delta > 0$ and a matrix $A \in \mathbb{C}^{m\times n}$, we will write $\mathrm{rk}_\delta(A)$ to denote the nonnegative integer determined by the expression*

$$\mathrm{rk}_\delta(A) = \sum_{j=1}^{\min\{m,n\}} H_\delta(s_j(A)),$$

where the numbers $s_j(A)$ represent the singular values corresponding to an economy-sized singular value decomposition of the matrix A.

Lemma III.2. *We will have that $\mathrm{rk}_\delta\left(A^\top\right) = \mathrm{rk}_\delta(A)$ for each $\delta > 0$ and each $A \in \mathbb{C}^{m\times n}$.*

Proof. Given an economy-sized singular value decomposition

$$U \begin{bmatrix} s_1(A) & & & \\ & s_2(A) & & \\ & & \ddots & \\ & & & s_{\min\{m,n\}}(A) \end{bmatrix} V = A$$

we will have that

$$V^\top \begin{bmatrix} s_1(A) & & & \\ & s_2(A) & & \\ & & \ddots & \\ & & & s_{\min\{m,n\}}(A) \end{bmatrix} U^\top = A^\top$$

is an economy-sized singular value decomposition of $A^\top$. This implies that

$$\mathrm{rk}_\delta\left(A^\top\right) = \sum_{j=1}^{\min\{m,n\}} H_\delta(s_j(A)) = \mathrm{rk}_\delta(A)$$

and this completes the proof. □

Lemma III.3. *Given $\delta > 0$ and $A \in \mathbb{C}^{m\times n}$ we will have that $\mathrm{rk}_\delta(A) \leq \mathrm{rk}(A)$.*

Proof. We will have that $\mathrm{rk}(A) = \sum_{j=1}^{\min\{m,n\}} H_0(s_j(A)) \geq \sum_{j=1}^{\min\{m,n\}} H_\delta(s_j(A)) = \mathrm{rk}_\delta(A)$. This completes the proof. □

Theorem III.4. *Given $\delta > 0$ and $y, x_1, \ldots, x_m \in \mathbb{C}^n$, let*

$$X = \begin{bmatrix} | & | & & | \\ x_1 & x_2 & \cdots & x_m \\ | & | & & | \end{bmatrix}.$$

If $\mathrm{rk}_\delta(X) > 0$ and if we set $r = \mathrm{rk}_\delta(X)$ and $s_{n,m}(r) = \sqrt{r(\min\{m,n\} - r)}$ then, there are a rank r orthogonal projector Q, r vectors $x_{j_1}, \ldots, x_{j_r} \in \{x_1, \ldots, x_m\}$ and r scalars $c_1 \ldots, c_r \in \mathbb{C}$ such that $\|X - QX\|_F \leq (s_{n,m}(r)/\sqrt{r})\delta$, and $\|y - \sum_{k=1}^r c_k x_{j_k}\| \leq \left(\sum_{k=1}^r |c_k|^2\right)^{\frac{1}{2}} s_{n,m}(r)\delta + \|(I_n - Q)y\|$.

Proof. Let us consider an economy-sized singular value decomposition $USV = A$. If u_j denotes the j-column of U, let Q be the rank $r = \mathrm{rk}_\delta(A)$ orthogonal projector determined by the expression $Q = \sum_{j=1}^r u_j u_j^*$. It can be seen that

$$\begin{aligned} \|X - QX\|_F^2 &= \sum_{j=r+1}^{\min\{m,n\}} s_j(X)^2 \\ &\leq (\min\{m,n\} - r)\delta^2 = \frac{s_{n,m}(r)^2}{r}\delta^2. \end{aligned}$$

Consequently, $\|X - QX\|_F \leq \frac{s_{n,m}(r)}{\sqrt{r}}\delta$.

Let us set.

$$\hat{X} = \begin{bmatrix} | & | & & | \\ \hat{x}_1 & \hat{x}_2 & \cdots & \hat{x}_m \\ | & | & & | \end{bmatrix} = QX$$

$$\hat{X}_y = \begin{bmatrix} | & | & & | & | \\ \hat{x}_1 & \hat{x}_2 & \cdots & \hat{x}_m & \hat{y} \\ | & | & & | & | \end{bmatrix} = Q\begin{bmatrix} X & y \end{bmatrix}$$

Since by lemma III.3 $\mathrm{rk}(X) \geq \mathrm{rk}_\delta(X)$, we will have that $\mathrm{rk}(\hat{X}) = r = \mathrm{rk}_\delta(X) > 0$, and since we also have that $\hat{x}_1, \ldots, \hat{x}_m, \hat{y} \in \mathrm{span}(\{u_1, \ldots, u_r\})$, there are r linearly independent $\hat{x}_{j_1}, \ldots, \hat{x}_{j_r} \in \{\hat{x}_1, \ldots, \hat{x}_m\}$ such that $\mathrm{span}(\{u_1, \ldots, u_r\}) = \mathrm{span}(\{\hat{x}_{j_1}, \ldots, \hat{x}_{j_r}\})$, this in turn implies that $\hat{y} \in \mathrm{span}(\{\hat{x}_{j_1}, \ldots, \hat{x}_{j_r}\})$ and there are $c_1, \ldots, c_r \in \mathbb{C}$ such that $\hat{y} = \sum_{k=1}^r c_k \hat{x}_{j_k}$. It can be seen that for each $z \in \{x_1, \ldots, x_m\}$

$$\|z - Qz\| \leq \|X - QX\|_F \leq \frac{s_{n,m}(r)}{\sqrt{r}}\delta,$$

and this in turn implies that

$$\begin{aligned}\left\|y-\sum_{k=1}^{r}c_k x_{j_k}\right\| &= \left\|y-\sum_{k=1}^{r}c_k x_{j_k}-\left(\hat{y}-\sum_{k=1}^{r}c_k\hat{x}_{j_k}\right)\right\| \\ &= \left\|y-\sum_{k=1}^{r}c_k x_{j_k}-Q\left(y-\sum_{k=1}^{r}c_k x_{j_k}\right)\right\| \\ &\leq \left(\sum_{k=1}^{r}|c_k|^2\right)^{\frac{1}{2}} s_{n,m}(r)\delta+\|(I_n-Q)y\|.\end{aligned}$$

This completes the proof. □

As a direct implication of theorem III.4 one can obtain the following corollary.

Corollary III.5. *Given $\delta>0$, $A\in\mathbb{C}^{m\times n}$ and $y\in\mathbb{C}^m$. If $\mathrm{rk}_\delta(A)>0$ and if we set $r=\mathrm{rk}_\delta(A)$ and $s_{n,m}(r)=\sqrt{r(\min\{m,n\}-r)}$ then, there are $x\in\mathbb{C}^n$ and a rank r orthogonal projector Q that does not depend on y, such that $\|Ax-y\|\leq\|x\|s_{n,m}(r)\delta+\|(I_m-Q)y\|$ and x has at most r nonzero entries.*

Proof. Let us set $x=\mathbf{0}_{n,1}$ and $a_j=A\hat{e}_{j,n}$ for $j=1,\ldots,n$. Since $r=\mathrm{rk}_\delta(A)>0$ and $s_{n,m}(r)=\sqrt{r(\min\{m,n\}-r)}$, by theorem III.4 we will have that there is a rank r orthogonal projector Q such that $\|A-QA\|_F\leq(s_{n,m}(r)/\sqrt{r})\delta$, and without loss of generality r vectors $a_{j_1},\ldots,a_{j_r}\in\{a_1,\ldots,a_n\}$ and r scalars $c_1\ldots,c_r\in\mathbb{C}$ with $j_1\leq j_2\leq\cdots\leq j_r$ (reordering the indices j_k if necessary), such that $\|y-\sum_{k=1}^r c_k a_{j_k}\|\leq\left(\sum_{k=1}^r|c_k|^2\right)^{\frac{1}{2}}s_{n,m}(r)\delta+\|(I_m-Q)y\|$. If we set $x_{j_k}=c_k$ for $k=1,\ldots,r$, we will have that $\|x\|=\left(\sum_{k=1}^r|c_k|^2\right)^{\frac{1}{2}}$ and $Ax=\sum_{k=1}^r x_{j_k}a_{j_k}=\sum_{k=1}^r c_k a_{j_k}$. Consequently, $\|Ax-y\|\leq\|x\|s_{n,m}(r)\delta+\|(I_m-Q)y\|$. This completes the proof. □

The results and ideas presented in this section can be translated into a sparse linear least squares solver algorithm described by algorithm A.1 in §IV.

B. Sparse structured nonlinear regressive model identification

Given time series data sets $\Sigma_x=\{x_t\}_{t\geq1}$ and $\Sigma_y=\{y_t\}_{t\geq1}$ in R^n corresponding to the orbits of two discrete-time dynamic financial systems of interest, let us consider the problem of identifying a map $\mathscr{T}$ relating the time series data according to the expression

$$y_t=\mathscr{T}(x_t)+r_t, \tag{III.2}$$

where r_t is some suitable small residual term defined as in (III.1). One may need to preprocess the time series data before proceeding with the approximate representation of a suitable evolution operator. For this purpose, given some prescribed integer $L>0$, one can consider the time series $\mathscr{D}_L(\Sigma_x)$ and $\mathscr{D}_L(\Sigma_y)$ determined by the expressions.

$$\begin{aligned}\mathscr{D}_L(\Sigma_x)&=\{\mathbf{x}_L(t)\}_{t\geq L}\\ \mathscr{D}_L(\Sigma_y)&=\{\mathbf{y}_L(t)\}_{t\geq L}\end{aligned}$$

For the dilated time series $\mathscr{D}_L(\Sigma_x)$ and $\mathscr{D}_L(\Sigma_y)$, the identification process corresponding to the relation (III.15), can be translated into the approximate solution of equations of the form

$$\mathbf{y}_L(t)=\tilde{\mathscr{T}}(\mathbf{x}_L(t)), \tag{III.3}$$

for $t\geq L$. Where $\tilde{\mathscr{T}}$ is the mapping to be approximately identified.

For any $p\geq1$, let us consider the map $\eth_p:\mathbb{R}^n\to\mathbb{R}^{d_p(n)}$ for $d_p(n)=n(n^p-1)/(n-1)+1$, that is determined by the expression.

$$\eth_p(x):=\begin{bmatrix}\Pi_1(x)\\ \Pi_2(x)\\ \vdots\\ \Pi_p(x)\\ 1\end{bmatrix}=\begin{bmatrix}x^{\otimes1}\\ x^{\otimes2}\\ \vdots\\ x^{\otimes p}\\ 1\end{bmatrix}$$

Given integers $p,L>0$, and two orbits $\Sigma_x=\{x_t\}_{t\geq1}$ and $\Sigma_y=\{y_t\}_{t\geq1}$ in $\mathbb{R}^n$, corresponding to two related dynamic financial processes of interest. For finite samples $\Sigma_N^x=\{x_t\}_{t=1}^T\subset\Sigma_x$ and $\Sigma_N^y=\{y_t\}_{t=1}^T\subset\Sigma_y$, let us consider the matrices:

$$\begin{aligned}\mathbf{H}_L^{(0,p)}(\Sigma_T^x)&=\begin{bmatrix}\eth_p(\mathbf{x}_L(L)) & \cdots & \eth_p(\mathbf{x}_L(T))\end{bmatrix}\\ \mathbf{H}_L^{(1)}(\Sigma_T^y)&=\begin{bmatrix}\mathbf{y}_L(L) & \cdots & \mathbf{y}_L(T)\end{bmatrix}\end{aligned} \tag{III.4}$$

The mapping identification mechanism used in this study for dilated systems of the form (III.3), will be approximately described by the expression:

$$\mathbf{y}_L(t)=\mathscr{T}(\mathbf{x}_L(t))=W\eth_p(\mathbf{x}_L(t)),\ t\geq L, \tag{III.5}$$

for some matrix $W\in\mathbb{R}^{n\times d_p(n)}$ to be determined, with $d_p(n)=n(n^p-1)/(n-1)+1$. Applying the techniques and ideas previously presented in this section, the matrix W in (III.5) can be estimated by approximately solving the matrix equation

$$W\mathbf{H}_L^{(0,p)}(\Sigma_T^x)=\mathbf{H}_L^{(1)}(\Sigma_T^y). \tag{III.6}$$

The devices described by (III.5) are called regressive reservoir computers (RRC) in this paper.

For any given integers $L,n,p>0$. Taking advantage of the maps $\eth_p$, one can find an integer $0<r_p(n)<d_p(n)$ together with a sparse matrix $R_{p,L}(n)\in\mathbb{R}^{r_p(n)\times d_p(n)}$, such that $R_{p,L}(n)^+R_{p,L}(n)\eth_p(x)\approx\eth_p(x)$ for $x\in\mathbb{R}^{nL}$. The existence of the pair $r_p(n),R_{p,L}(n)$ is determined by the following theorem.

Theorem III.6. *Given $\varepsilon\in\mathbb{R}^+$ and $L,n,p\in\mathbb{Z}^+$. There are an integer $0<\rho_p(n)<d_p(n)$ and a sparse matrix $R_{p,L}(n)\in\mathbb{R}^{\rho_p(n)\times d_p(n)}$ with $d_p(n)$ nonzero entries, such that $\|R_{p,L}(n)^+R_{p,L}(n)\eth_p(x)-\eth_p(x)\|\leq\sqrt{d_p(nL)}\varepsilon$ for each $x\in\mathbb{R}^{nL}$.*

Proof. Let us consider the symmetric group $\mathfrak{S}_{nL-1}$ on $nL-1$ letters, and let us consider any finite set of distinct points

$\{\hat{x}_1,...,\hat{x}_{nL},\hat{x}_{nL+1}\} \subset \mathbb{R}$ such that for each $1 \leq m \leq p$ and every pair on index sets $\{i_1,\ldots,i_m\},\{j_1,\ldots,j_m\} \subset \{1,\ldots,nL+1\}$:

$$\prod_{k=1}^{m} \hat{x}_{j_k} = \prod_{k=1}^{m} \hat{x}_{i_k}, \Leftrightarrow \exists \sigma \in \mathfrak{S}_{nL-1} : i_k = \sigma(j_k), \forall 1 \leq k \leq m. \tag{III.7}$$

That is, the previously considered products coincide if and only if, the index set $\{i_1,\ldots,i_m\}$ is a permutation of the set $\{j_1,\ldots,j_m\}$, for each $1 \leq m \leq p$.

Let us now set $\mathbf{y} = \nu\left[\hat{x}_1 \;\; \hat{x}_2 \;\; \cdots \;\; \hat{x}_{nL}\right]^\top$, $d = d_p(n)$ and

$$\tilde{\mathbf{x}} = \left[\tilde{x}_1 \;\; \cdots \;\; \tilde{x}_d\right]^\top := \eth_p(\mathbf{y}).$$

If in addition we consider the following assignments:

$$\tilde{x}_d := \hat{x}_{nL+1},$$

$$R = e_{1,d}^\top.$$

Then, for each $j = 2,\ldots,d$ one can find $1 \leq k_1(j),\ldots,k_{n_j}(j) \leq d$ such that $|\tilde{x}_j - \tilde{x}_{k_m(j)}| \leq \varepsilon$, for every $1 \leq m \leq n_j$. Consequently, if we set $R_0 := (1/n_j)\sum_{l=1}^{n_j} \hat{e}_{k_l(j),d}^T$ and

$$R := \begin{bmatrix} R \\ R_0 \end{bmatrix},$$

whenever $k_1(j) = j$. After iterating on the previously described procedure for $2 \leq j \leq d$, we can define $R_{p,L}(n) := R$ and we can set the value of $\rho_p(n)$ as the number of rows of $R_{p,L}(n)$.

Given $x \in \mathbb{R}^{nL}$. Based on the structure of $R_{p,L}(n)$ determined by the constructive procedure used for its computation, it can be verified that $R_{p,L}(n)^+$ is well defined and in addition:

$$\|R_{p,L}(n)^+ R_{p,L}(n)\eth_p(x) - \eth_p(x)\| \leq \sqrt{d_p(n)}\varepsilon.$$

This completes the proof. □

In order to reduce to computational effort corresponding to the solution of (III.6), using the matrix $R_{p,L}(n)$ described by Theorem III.6, one can obtain an approximate reduced representation of (III.6) determined by the expression.

$$\bar{W} R_{p,L}(n) \mathbf{H}_L^{(0,p)}(\Sigma_T^x) = \mathbf{H}_L^{(1)}(\Sigma_T^y) \tag{III.8}$$

The architecture of the regressive reservoir computers considered in this study was inspired by next generation reservoir computers[10].

Schematically, the regressive models considered in this study can be described by a block diagram of the form,

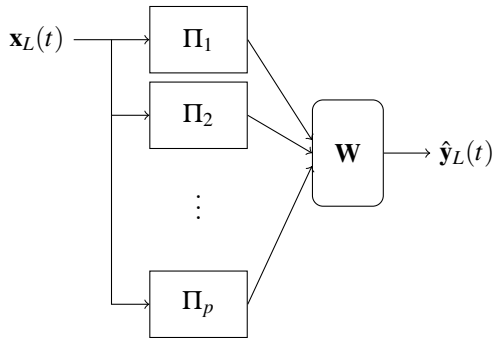

(III.9)

where for each $t \geq L$, the block $\mathbf{W}$ is determined by the expression

$$\begin{aligned}\mathbf{W}(\Pi_1(\mathbf{x}_L(t)),\ldots,\Pi_p(\mathbf{x}_L(t))) &:= \tilde{W}\begin{bmatrix}\Pi_1(\mathbf{x}_L(t)) \\ \vdots \\ \Pi_p(\mathbf{x}_L(t))\end{bmatrix} + c_W \\ &= \begin{bmatrix}\tilde{W} & c_W\end{bmatrix} \eth_p(\mathbf{x}_L(t))\end{aligned}$$

and where the matrix $W = \begin{bmatrix}\tilde{W} & c_W\end{bmatrix}$ is determined by (III.6).

The structure of the generic block $\mathbf{W}$ ub (III.9) can be factored in the form

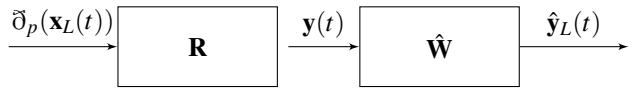

(III.10)

The layers $\mathbf{R}$ and $\hat{\mathbf{W}}$ of the device (III.10) are determined by the expressions

$$\mathbf{R}(\mathbf{x}) = \hat{R}\mathbf{x},$$
$$\hat{\mathbf{W}}(\mathbf{y}) = W\mathbf{y}$$

for any pair of suitable vectors $\mathbf{x},\mathbf{y}$. Where W is a sparse representation of an approximate solution to (III.8) and $\hat{R}$ is determined by Theorem III.6.

Using the reservoir computer models described by (III.5), (III.9) and (III.10), we can compute approximate representations of the mappings that satisfy (III.3) using the expression

$$\begin{aligned}\hat{\mathscr{T}}(\mathbf{x}_L(t)) &:= \hat{K}\left(\hat{\mathbf{W}} \circ \mathbf{R} \circ \eth_p(\mathbf{x}_L(t)\right) \\ &= \hat{K}W\hat{R}\eth_p(\mathbf{x}_L(t))),\end{aligned} \tag{III.11}$$

for each $t \geq L$, with

$$\hat{K} = \begin{bmatrix} \hat{e}_{1,nL}^\top \\ \hat{e}_{L+1,nL}^\top \\ \vdots \\ \hat{e}_{(n-1)L+1,nL}^\top \end{bmatrix}.$$

Furthermore, we can use the identified RRC model $\hat{\mathscr{T}}$ to simulate the behavior $y_t = \mathscr{T}(x_t)$ of the system described by (III.15) for $L \leq t \leq \tau$, by performing the operation:

$$\mathbf{T}(\mathbf{x}_L(t)) := \hat{K}\hat{\mathscr{T}}(\mathbf{x}_L(t)) = \hat{K}W\eth_p(\mathbf{x}_L(t))), \tag{III.12}$$

for some suitable $\tau > 0$.

Theorem III.7. *Given $\delta > 0$, two integers $p,L > 0$, a sample $\Sigma_T = \{x_t\}_{t=1}^T$ from a dynamic financial system's orbit $\Sigma = \{x_t\}_{t\geq 1} \subset \mathbb{R}^n$ with $T > L$, and a matrix solvent $\bar{W} \in \mathbb{R}^{nL\times r_p(nL)}$ of* (III.8) *with $R_{p,L}(n)$ and $r_p(n)$ determined by Theorem III.6. If $r = \mathrm{rk}_\delta(R_{p,L}(n)\mathbf{H}_L^{(0,p)}(\Sigma_T)) > 0$, then there is a sparse representation $\hat{W} \in \mathbb{R}^{nL\times\rho_p(nL)}$ of $\bar{W}$ with at most $r\rho_p(nL)$ nonzero entries such that*

$$\|\hat{W}R_{p,L}(n)\mathbf{H}_L^{(0,p)}(\Sigma_T) - \bar{W}R_{p,L}(n)\mathbf{H}_L^{(0,p)}(\Sigma_T)\|_F \leq K\delta, \tag{III.13}$$

for $K = \sqrt{nL(\min\{\rho_p(nL),T-L\}-r)}(\sqrt{r}\|\hat{W}\|_F + \|\bar{W}\|_F)$, where $\rho_p(nL)$ is the integer described by Theorem III.6.

Proof. Let us set $H = R_{p,L}(n)\mathbf{H}_{L,G}^{(0,p)}(\Sigma_T)^\top$ and $Y = H\bar{W}^\top$. It suffices to prove that there is a sparse representation $\hat{W} \in \mathbb{R}^{nL\times\rho_p(nL)}$ with at most $r\rho_p(nL)$ nonzero entries such that

$$\|H\hat{W}^\top - Y\|_F \leq K\delta.$$

Since we have that

$$\begin{aligned}\mathrm{rk}_\delta(H) &= \mathrm{rk}_\delta\left(\left(R_{p,L}(n)\mathbf{H}_{L,G}^{(0,p)}(\Sigma_T)\right)^\top\right)\\ &= \mathrm{rk}_\delta(R_{p,L}(n)\mathbf{H}_{L,G}^{(0,p)}(\Sigma_T)) > 0\end{aligned}$$

by Lemma III.2. By Corollary III.5, if we set $r = \mathrm{rk}_\delta(H)$ and $\alpha = \sqrt{r(\min\{\rho_p(nL), T-L\}-r)}$. We will have that there is a rank r orthogonal projector Q such that for each $j = 1,\ldots,nL$, there is $\hat{v}_j \in \mathbb{R}^{nL}$ with at most r nonzero entries, for which $\|H\hat{v}_j - Y\hat{e}_{j,M}\| \leq \alpha\|\hat{v}_j\|\delta + \|(I_{T-L}-Q)Y\hat{e}_{j,nL}\|$. Consequently, if we set

$$\hat{W} = \begin{bmatrix} | & & | \\ \hat{v}_1 & \cdots & \hat{v}_{nL} \\ | & & | \end{bmatrix}^\top$$

we will have that $\hat{W}$ has at most nrL nonzero entries and

$$\begin{aligned}\|H\hat{W}^\top - Y\|_F^2 &= \sum_{j=1}^{nL}\|H\hat{v}_j - Y\hat{e}_{j,nL}\|^2\\ &\leq M(\alpha\|\hat{W}\|_F\delta + \|(I_{T-L}-Q)Y\|_F)^2,\end{aligned}$$

and this in turn implies that,

$$\|H\hat{W}^\top - Y\|_F \leq \sqrt{nL}(\alpha\|\hat{W}\|_F\delta + \|(I_{T-L}-Q)H\|_F\|\bar{W}\|_F). \tag{III.14}$$

By (III.14) and by Theorem III.4 we will have that

$$\begin{aligned}\|H\hat{W}^\top - Y\|_F &\leq \sqrt{nL}(\alpha\|\hat{W}\|_F\delta + (\alpha/\sqrt{r})\|\bar{W}\|_F\delta)\\ &= \alpha\sqrt{(nL/r)}(\sqrt{r}\|\hat{A}\|_F + \|A\|_F)\delta = K\delta.\end{aligned}$$

This completes the proof. □

1. Sparse structured nonlinear autoregressive model identification

Given some time series data $\Sigma \subset \mathbb{R}^n$ corresponding to an orbit determined by the difference equation

$$x_{t+1} = \mathscr{A}(x_t), \tag{III.15}$$

for some discrete-time dynamic financial model $(\hat{\mathbf{\Sigma}}, \mathscr{T})$ to be identified. One can use the methods presented in §III B to identify the mapping $\mathscr{S}$, by considering the RRC model identification determined by the problem

$$y_t = \mathscr{A}(x_t),$$

for the time series $\Sigma_x := \{x_t\}_{t\geq 1}$ and $\Sigma_y := \{y_t\}_{t\geq 1}$ in $\mathbb{R}^n$, with $y_t := x_{t+1}$ for each $t \geq 1$.

IV. ALGORITHMS

The sparse model identification methods presented in §III A can be translated into prototypical algorithms that will be presented in this section, some programs for data reading and writing, synthetic signals generation, and predictive simulation are also included as part of the **DyNet** tool-set available in[15].

A. Sparse linear least squares solver and structured assembling matrix identification algorithms

As an application of the results and ideas presented in §III A one can obtain a prototypical sparse linear least squares solver algorithm like algorithm A.1.

The least squares problems $c = \arg\min_{\hat{c}\in\mathbb{C}^K}\|\hat{A}\hat{c} - y\|$ to be solved as part of the process corresponding to algorithm A.1 can be solved with any efficient least squares solver available in the language or program where the sparse linear least squares solver algorithm is implemented. For the Python version of algorithm A.1 the function `lstsq` is implemented.

In this section, we focus on the applications of the structured matrix approximation methods presented in SIII, to dynamical financial systems identification via regressive reservoir computers.

B. Structured coupling matrix identification algorithm

Given a discrete-time dynamic financial model $(\Sigma, \mathscr{T})$ and a structured data sample $\Sigma_T \subset \Sigma$, we can apply Algorithm A.2 and Algorithm A.1, in order to compute the output coupling matrix that can be used to obtain an approximate representation of the evolution operator $\mathscr{T}$, corresponding to the orbit Σ. For this purpose, one can use the following Algorithm.

V. NUMERICAL SIMULATIONS

In this section, we will present some numerical simulations computed using the **DyNet** toolset available in[15], which was developed as part of this project. The toolset consists of a collection of Python 3.9.13 for structured sparse identification and numerical simulation of discrete-time dynamical financial systems.

The numerical experiments documented in this section were performed with Python 3.9.13. All the programs written for real-world data reading, synthetic data generation, and sparse model identification as part of this project are available at[15].

The numerical simulations reported in this section were computed on Windows 11 Enterprise PC equipped with AMD Ryzen 5 3450U 2.10 GHz processor and with 8.00 GB RAM.

Algorithm A.1 SLRSolver: Sparse linear least squares solver algorithm

Data: $A \in \mathbb{C}^{m\times n}$, $Y \in \mathbb{C}^{m\times p}$, $\delta > 0$, $N \in \mathbb{Z}^+$, $\varepsilon > 0$
Result: $X = \textbf{SLRSolver}(A, Y, \delta, N, \varepsilon)$

1. Compute economy-sized SVD $USV = A$
2. Set $s = \min\{m,n\}$
3. Set $r = \mathrm{rk}_\delta(A)$
4. Set $U_\delta = \sum_{j=1}^{r} U\hat{e}_{j,s}\hat{e}_{j,s}^*$
5. Set $T_\delta = \sum_{j=1}^{r} (\hat{e}_{j,s}^* S \hat{e}_{j,s})^{-1} \hat{e}_{j,s}\hat{e}_{j,s}^*$
6. Set $V_\delta = \sum_{j=1}^{r} \hat{e}_{j,s}\hat{e}_{j,s}^* V$
7. Set $\hat{A} = U_\delta^* A$
8. Set $\hat{Y} = U_\delta^* Y$
9. Set $X_0 = V_\delta^* T_\delta \hat{Y}$
10. **for** $j = 1, \ldots, p$ **do**
    Set $K = 1$
    Set error $= 1 + \delta$
    Set $c = X_0 \hat{e}_{j,p}$
    Set $x_0 = c$
    Set $\hat{c} = \begin{bmatrix} \hat{c}_1 & \cdots & \hat{c}_n \end{bmatrix}^\top = \begin{bmatrix} |\hat{e}_{1,n}^* c| & \cdots & |\hat{e}_{n,n}^* c| \end{bmatrix}^\top$
    Compute permutation $\sigma : \{1,\ldots,n\} \to \{1,\ldots,n\}$ such that: $\hat{c}_{\sigma(1)} \geq \hat{c}_{\sigma(2)} \geq \cdots \geq \hat{c}_{\sigma(n)}$
    Set $N_0 = \max\left\{\sum_{j=1}^{n} H_\varepsilon\left(\hat{c}_{\sigma(j)}\right), 1\right\}$
    while $K \leq N$ **and** error $> \delta$ **do**
        Set $x = \mathbf{0}_{n,1}$
        Set $A_0 = \sum_{j=1}^{N_0} \hat{A}\hat{e}_{\sigma(j),n}\hat{e}_{j,N_0}^*$
        Solve $c = \arg\min_{\tilde{c}\in\mathbb{C}^{N_0}} \|A_0\tilde{c} - \hat{Y}\hat{e}_{j,p}\|$
        for $k = 1, \ldots, N_0$ **do**
            Set $x_{\sigma(k)} = \hat{e}_{k,N_0}^* c$
        end for
        Set error $= \|x - x_0\|_\infty$
        Set $x_0 = x$
        Set $\hat{c} = \begin{bmatrix} \hat{c}_1 & \cdots & \hat{c}_n \end{bmatrix}^\top = \begin{bmatrix} |\hat{e}_{1,n}^* x| & \cdots & |\hat{e}_{n,n}^* x| \end{bmatrix}^\top$
        Compute permutation $\sigma : \{1,\ldots,n\} \to \{1,\ldots,n\}$ such that: $\hat{c}_{\sigma(1)} \geq \hat{c}_{\sigma(2)} \geq \cdots \geq \hat{c}_{\sigma(n)}$
        Set $N_0 = \max\left\{\sum_{j=1}^{n} H_\varepsilon\left(\hat{c}_{\sigma(j)}\right), 1\right\}$
        Set $K = K + 1$
    end while
    Set $x_j = x$
11. **end for**
12. Set $X = \begin{bmatrix} | & | & & | \\ x_1 & x_2 & \cdots & x_p \\ | & | & & | \end{bmatrix}$

return X

Algorithm A.2 Compression matrix computation algorithm

Data: $n, p, L \in \mathbb{Z}^+$, $\nu, \varepsilon \in \mathbb{R}^+$.
Result: COMPRESSION MATRIX FACTOR: $R_{p,L}(n)$

1. Choose nL pseudorandom numbers $\hat{x}_1, \ldots, \hat{x}_{nL} \in \mathbb{R}$ from $N(0,1)$
2. Set $\mathbf{y} = \nu \begin{bmatrix} \hat{x}_1 & \hat{x}_2 & \cdots & \hat{x}_{nL} \end{bmatrix}^\top$
3. Set $d = d_p(n)$
4. Set $\tilde{\mathbf{x}} = \begin{bmatrix} \tilde{x}_1 & \cdots & \tilde{x}_d \end{bmatrix}^\top := \eth_p(\mathbf{y})$
5. Choose a pseudorandom number $\alpha \in N(0,1)$;
6. Set $\tilde{x}_d := \alpha$
7. Set $R = e_{1,d}^\top$
8. **for** $j = 2, \ldots, d$ **do**
    Find $1 \leq k_1, \ldots, k_{n_j} \leq d$ such that $|\tilde{x}_j - \tilde{x}_{k_m}| \leq \varepsilon$, for each $1 \leq m \leq n_j$
    if $k_1 = j$ **then**
        Set $R_0 := (1/n_j) \sum_{l=1}^{n_j} \hat{e}_{k_l,d}^T$
        Set $R := \begin{bmatrix} R \\ R_0 \end{bmatrix}$
    end if
9. **end for**
10. Set $R_{p,L}(n) := R$

return $R_{p,L}(n)$

Algorithm B.1 RRC Model: RRC model identification

Data: $\Sigma_N^x = \{x_t\}_{t=1}^T, \Sigma_N^y = \{y_t\}_{t=1}^T \subset \mathbb{R}^n$
Result: OUTPUT COUPLING AND COMPRESSION MATRICES: $\hat{W}, \tilde{W}, R_{p,L}(n)$

1. Choose or estimate the lag value L using auto-correlation function based methods
2. Set a tensor order value p
3. Compute compression matrix $R_{p,L}(n)$ applying Algorithm A.2
4. Compute matrices:

$$\mathbf{H}_0 := \mathbf{H}_L^{(0,p)}(\Sigma_T^x)$$
$$\mathbf{H}_1 := \mathbf{H}_L^{(1)}(\Sigma_T^y)$$

5. Approximately solve:

$$\hat{W}\left(R_{p,L}(n)\mathbf{H}_0\right) = \mathbf{H}_1$$

for $\hat{W}$ applying Algorithm A.1

return $\hat{W}, R_{p,L}(n)$

A. Sparse autoregressive reservoir computers for dynamical nonlinear financial system behavior identification

In this section, we consider a nonlinear dynamical financial system described by the model

$$\begin{aligned}
\dot{x}_1 &= x_3 + (x_2 - s)x_1, \\
\dot{x}_2 &= 1 - cx_2 - x_1^2, \\
\dot{x}_2 &= -x_1 - ex_3, \\
x_1(0) &= x_0, x_2(0) = y_0, x_3(0) = z_0.
\end{aligned} \tag{V.1}$$

As observed in[4], systems of the form (V.1) can exhibit, among others behavior types, chaotic and eventually approximately periodic dynamic behavior depending on the configuration of parameters and initial conditions considered for (V.1).

1. *Chaotic behavior identification*

For $s = 3, c = 0.1, e = 1$, let us consider the initial conditions $x_0 = 2, y_0 = 3, z_0 = 2$. For this configuration, one can obtain synthetic time series data $\Sigma_{12000} \subset \mathbb{R}^3$ obtained by applying a fourth-order adaptive numerical integration method to (V.1) for the configuration determined by the previous choice of parameters, obtaining an orbit's samples set Σ_{12000} whose elements are uniformly distributed with respect to the time interval [0,120].

The training orbit's data set corresponding to the first 50% of the data in Σ_{12000}, together with the remaining data used for model validation, are illustrated in Figure 1. The factorization for the output coupling matrix $W = \hat{W}R$ determined by Theorems III.6 and III.7 are illustrated in Figure 2.

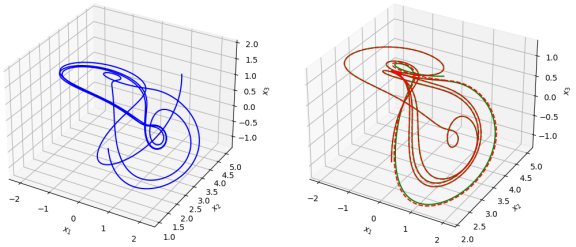

Figure 1: Training orbits data (left), validation orbits data (right). The green line corresponds to validation data, and the red dotted line corresponds to the model's predictions.

2. *Eventually approximately periodic behavior identification*

For $s = 0.5, c = 0.1, e = 0.1$, let us consider the initial conditions $x_0 = 1, y_0 = 1, z_0 = 1$. For this configuration, one can obtain synthetic time series data $\Sigma_{12000} \subset \mathbb{R}^3$ obtained by applying a fourth-order adaptive numerical integration method to (V.1) for the configuration determined by the previous choice of parameters, obtaining an orbit's samples set Σ_{12000} whose elements are uniformly distributed with respect to the time interval [0,120].

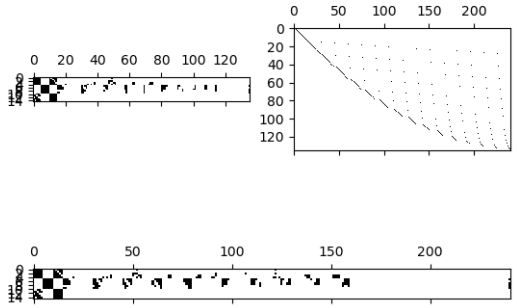

Figure 2: Matrix factors $\hat{W}$ (top-left) and R (top-right), output coupling matrix $W = \hat{W}R$ (bottom).

The training orbit's data set corresponding to the first 6.67% of the data in Σ_{12000}, together with the remaining data used for model validation, are illustrated in Figure 3. The factorization for the output coupling matrix $W = \hat{W}R$ determined by Theorems III.6 and III.7 are illustrated in Figure 4.

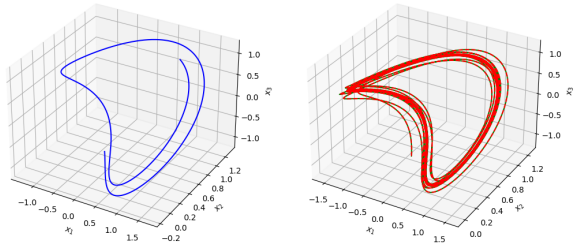

Figure 3: Training orbits data (left), validation orbits data (right). The green line corresponds to validation data, and the red dotted line corresponds to the model's predictions.

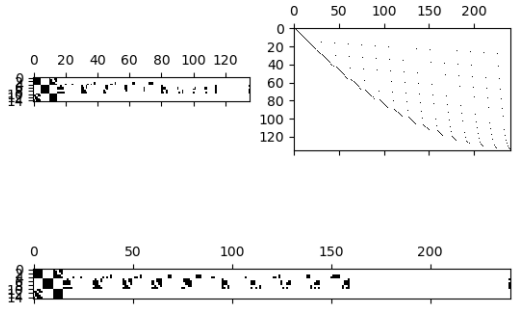

Figure 4: Matrix factors $\hat{W}$ (top-left) and R (top-right), output coupling matrix $W = \hat{W}R$ (bottom).

The computational setting used for the experiments performed in this section is documented in the Python 3.9.13 program `FDSExperiment.py` in[15] that can be used to replicate these results.

B. Sparse network based representation of dynamic financial remittances distribution processes

The influx of remittances contributes to the economic stability of recipient countries, as they have a countercyclical behavior[6,8]. Under the nuanced lens of economic analysis[12], it is deduced that nations with a heightened ratio of remittances to GDP concurrently exhibit a substantially increased average ratio of deposits to GDP. This deduction stands in contrast to countries characterized by lower remittance-to-GDP ratios.

In addition, it has been observed that remittances contribute to the financial system development, increasing banks capacity to mobilize savings and lend funds[3]. Although a high portion of remittances are paid by the formal system, the influx of remittances through the informal system can have an impact in banks balance sheets, as a result of the transaction needs of the economic agents[7].

Remittances can potentially boost deposits, augmenting disposable resources within recipient zones. Whether these resources remain in the banking accounts of recipients or are utilized for transactions with banked individuals, a lasting increase in bank deposits could be anticipated[1].

In particular, for the Honduran economy, remittances play an important role, in energizing consumption, savings, and investments. In 2021, remittances represented 25.3% of GDP[5], and deposits represented 64.8% of GDP. In January 2023, 71.7% of remittances received were collected in cash at remittance service providers, 10.5% through mobile apps, and 17.5% through deposits into banking accounts[2].

In the Honduran economic landscape, remittances have emerged as a pivotal financial resource, contributing significantly with a substantial 43.5% share of households' overall income. Notably, 87.4% of these remittance resources are earmarked to cover essential needs, spanning living expenses, educational pursuits, and medical treatments. Furthermore, 7.5% is strategically allocated towards the acquisition or enhancement of fixed assets.

For the examples documented in this section, we have used anonymized and synthesized data based on real information on deposits and remittances from the Honduran financial system, that are recorded by the National Commission of Banks and Insurance Companies (**CNBS**) quarterly, and were collected between 2017 and 2022.

The main motivation for the model identification considered in this section is the estimation of an empirical measure of exposure to remittances influx of the deposits in 15 key institutions of the Honduran financial system.

The models considered in this section were trained with the first 95% of the data in the time series' sample. The experiments in this section center on the time series of remittance inflows for 18 Honduran regions and the deposits of 15 key institutions in the Honduran financial system. These time series cover the period from 2017 to 2022.

For the experiments documented in this section, the variable t denotes the number of quarters t after the first quarter of 2017. The remittances and deposits signals used for the experiments reported in this section have been re-scaled preserving proportions, as part of the anonymization process applied to the financial time series considered for this study. For this study $\mathbf{r}(t) = [r_k(t)] \in \mathbb{R}^{18}$ represents a vector of remittances influx signals at time step t with $r_k(t)$ representing the remittance influx for the geographic region $1 \leq k \leq 18$ at time step t.

Let $\mathbf{d}(t) := [d_j(t)] \in \mathbb{R}^{15}$ represent the vector of deposits signals at time step t, with $d_j(t)$ denoting the deposits in institution $1 \leq j \leq 15$ at time step t. The empirical measure of exposure $\mathscr{E}_j$ considered for this study is determined for each $1 \leq j \leq 15$ by the following expression.

$$\mathscr{E}_j(\mathbf{r},\mathbf{d}) := \frac{\sqrt{\sum_{t=0}^{T}(\hat{d_j}(t) - d_j(t))^2}}{\sqrt{T+1}\max\{|d_j(t)| : 0 \leq t \leq T\}}.$$

Where $\hat{\mathbf{d}}(t) := [\hat{d_j}(t)] \in \mathbb{R}^{15}$ denotes the estimated deposits (using models of the form (V.2) or (V.3)) corresponding to time step t and with $\hat{d_j}(t)$ representing the estimated deposits in institution $1 \leq j \leq 15$ at the time step t.

1. Non-lagged sparse RRC model

For this experiment, we are considering a composition of two sparse RRC models, obtaining a fully linear sparse regressive reservoir computer model determined by the expression

$$\hat{\mathbf{d}}(t) = KA\mathbf{r}(t) + \hat{\mathbf{w}}(t). \tag{V.2}$$

Where K represents the deposits estimation refinement matrix transformation, A denotes a remittances distribution dynamic matrix factor, and $\hat{\mathbf{w}}(t)$ represents an uncertainty factor.

The relational reference network corresponding to the model (V.2) is shown in the Figure 5. The top four most exposed institutions according to the model (V.2) are shown in Figure 6.

2. Lagged sparse RRC model

The following experiment is an extension of the model proposed in §V B 1. The data considered for this model includes both lagged and non-lagged remittances based signals, which allows an alternative remittances exposure identification strategy for the deposits in the financial system. For this exercise, a lagged sparse regressive reservoir computer model was

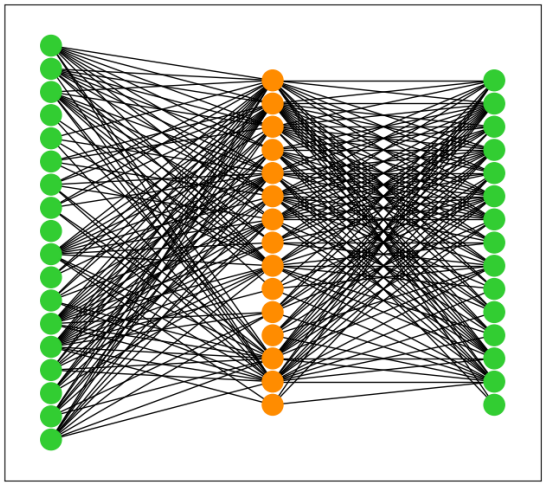

Figure 5: Relational reference network for the dynamic process model determined by (V.2).

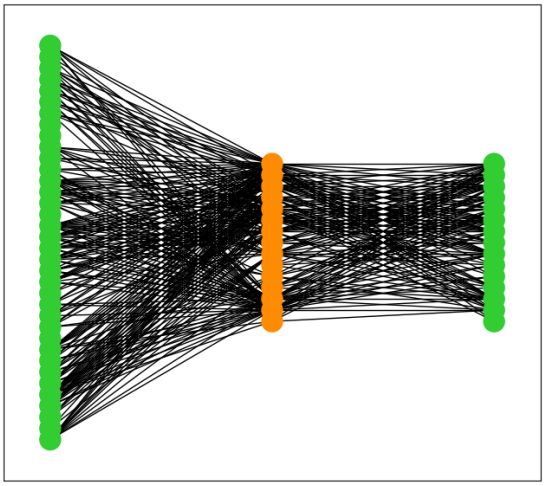

Figure 7: Relational reference network for the process estimate determined by (V.3)

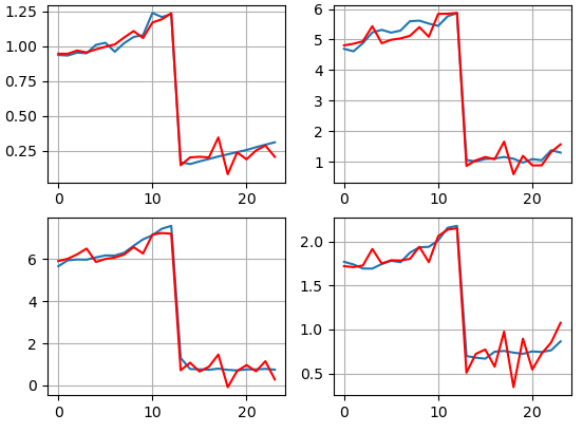

Figure 6: Reference signals (blue line) and model prediction (red line) computed with a sparse linear regression reservoir computer model for nodes d_10 (top left), d_9 (top right), d_6 (bottom left) and d_8 (bottom right).

used, which considers remittance flows at time steps t and $t-1$. This model is described by the expression

$$\hat{\mathbf{d}}(t) = \hat{K}\hat{A}\begin{bmatrix}\mathbf{r}(t)\\ \mathbf{r}(t-1)\end{bmatrix} + \hat{\mathbf{w}}(t). \tag{V.3}$$

Where $\hat{K}$ represents the deposits estimation refinement matrix factor, $\hat{A}$ denotes a remittances distribution dynamic matrix, and $\hat{\mathbf{w}}(t)$ represents the uncertainty factor.

The relational network for the model identified in this section is shown in Figure 7. The top four most exposed institutions according to the model (V.3) are shown in Figure 8.

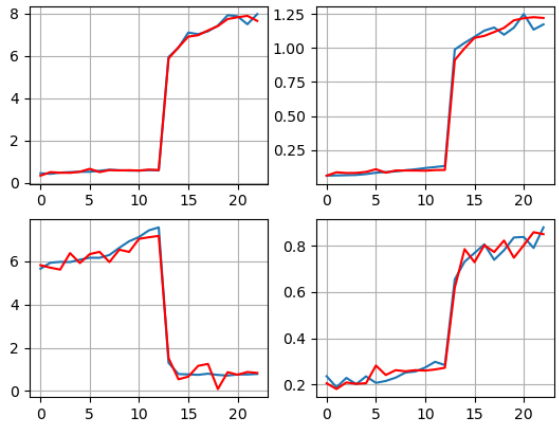

Figure 8: Reference signals (blue line) and model prediction (red line) computed with a sparse linear regression reservoir computer model for nodes d_{14} (top left), d_{11} (top right), d_6 (bottom left) and d_{15} (bottom right).

The combination of fully linear lagged and non-lagged sparse RRC models considered previously are aimed to provide an example of the potential that this model combination has to capture the levels of exposure to remittances flows of the deposits in the Honduran financial system.

The computational setting used for the experiments performed in this section is documented in the Python program `Simulation.py` in[15], and this program can be used to repli-

cate these experiments.

VI. CONCLUSIONS

The results in §III A and §III B in the form of algorithms like the ones described in §IV, can be effectively used for the sparse structured identification of financial dynamical models that can be used to compute data-driven predictive numerical simulations.

The synergy of the NRRCs models with sparse techniques allowed modeling of the relationship between remittance flows and deposits of the Honduran financial system, ensuring more accurate predictions of the dynamic behavior and interrelation of these variables.

The application of these models permitted the identification of the deposit's exposure of diverse institutions to the remittances inflows received in 18 geographic areas of the country.

VII. FUTURE DIRECTIONS

The extension of sparse RRC modeling techniques to equivariant system identification will be studied in future communications. Further implementations of the structured sparse model identification algorithms presented in this document to compute data-driven dynamic general equilibrium models will be the subject of future communications.

DATA AVAILABILITY

The programs and data that support the findings of this study will be openly available in the DyNet-CNBS repository, reference number[15], in due time.

CONFLICTS OF INTEREST

The authors declare that they have no conflicts of interest.

ACKNOWLEDGMENT

The structure preserving matrix computations needed to implement the algorithms in §IV, were performed with Python 3.9.13, with the support and computational resources of the National Commission of Banks and Insurance Companies (**CNBS**) of Honduras.

REFERENCES

[1] Banxico. Remesas, captación minorista y género. Technical report, Banco de México, 2022.

[2] BCH. Resultado semestral encuesta de remesas familiares enero 2023. Technical report, Banco Central de Honduras, 2023.

[3] R. Brown and F. Carmignani. Revisiting the effects of remittances on bank credit: A macro perspective. *Scottish Journal of Political Economy*, 62:454–485, 2015.

[4] Rajat Budhiraja, Manish Kumar, Mrinal K. Das, Anil Singh Bafila, and Sanjeev Singh. A reservoir computing approach for forecasting and regenerating both dynamical and time-delay controlled financial system behavior. *PLOS ONE*, 16(2):1–24, 02 2021.

[5] Elvis T. Casco. Remesas familiares en Honduras 2017-2022. Technical report, Banco Central de Honduras, 2023.

[6] R. Chami, A. Barajas, T. Comisano, C. Fullenkamp, M Gapen, and P. Montiel. Macroeconomic consequences of remittances. *IMF Occasional Paper*, pages 1–74, 2008.

[7] R. Chami, A. Barajas, C. Ebeke, and A. Oeking. What's different about monetary policy transmission in remittance-dependent countries? *IMF Working Paper*, pages 3–35, 2016.

[8] R. Chami, C. Fullenkamp, and M. Gapen. Measuring workers remittances: What should be kept in and what should be left out. *IMF Occasional Paper*, 2009.

[9] Matthew Dixon, Diego Klabjan, and Jin Hoon Bang. Classification-based financial markets prediction using deep neural networks, 2017.

[10] Daniel J. Gauthier, Erik Bollt, Aaron Griffith, and Wendson A. S. Barbosa. Next generation reservoir computing. *Nature Communications*, 12(1):5564, Sep 2021.

[11] Gene H. Golub and Charles F. Van Loan. *Matrix Computations*. The Johns Hopkins University Press, Baltimore, 3rd edition, 1996.

[12] D. Muktadir-Al-Mukit and N. Islam. Relationship between remittance and credit disbursement of the banking sector: A study from bangladesh. *Journal of Business and Management Research*, 1(1):39–52, 2016.

[13] Balasubramanya T. Nadiga. Reservoir computing as a tool for climate predictability studies. *Journal of Advances in Modeling Earth Systems*, 13(4):e2020MS002290, 2021. e2020MS002290 2020MS002290.

[14] Justin Sirignano and Rama Cont. Universal features of price formation in financial markets: perspectives from deep learning, 2018.

[15] Fredy Vides. Dynet-cnbs: Network dynamics identification and reservoir computing tools with financial applications. 2023. https://github.com/FredyVides/DyNet-CNBS.

[16] Ye Yuan, Xiuchuan Tang, Wei Zhou, Wei Pan, Xiuting Li, Hai-Tao Zhang, Han Ding, and Jorge Goncalves. Data driven discovery of cyber physical systems. *Nature Communications*, 10(1):4894, Oct 2019.